

Polyethylene glycol 400 enables plunge-freezing cryopreservation of human keratinocytes

Ivan Klbik^{a,b,*}, Katarína Čechová^c, Stanislava Milovská^d, Helena Švajdlenková^{e,h}, Igor Maňko^a, Ján Lakota^{f,g}, Ondrej Šauša^{a,h}

^a Institute of Physics SAS, 845 11 Bratislava, Slovak Republic

^b Department of Experimental Physics, FMFI, Comenius University, 842 48 Bratislava, Slovak Republic

^c Department of Nuclear Physics and Biophysics, FMFI, Comenius University, 842 48 Bratislava, Slovak Republic

^d Earth Science Institute SAS, 974 01 Banská Bystrica, Slovak Republic

^e Polymer Institute SAS, 845 41 Bratislava, Slovak Republic

^f Faculty of Management Comenius University, 820 05 Bratislava, Slovak Republic

^g Center of Experimental Medicine SAS, 841 04 Bratislava, Slovak Republic

^h Department of Nuclear Chemistry, FNS, Comenius University, 842 15 Bratislava, Slovak Republic

ARTICLE INFO

Article history:

Received 24 January 2023

Revised 11 March 2023

Accepted 21 March 2023

Available online 24 March 2023

Keywords:

Cryopreservation

Polyethylene glycol

Keratinocytes

Dimethyl sulfoxide

Microstructure

Positron annihilation

Thermal analysis

ABSTRACT

An effort was made to design a simple and efficient protocol for the cryopreservation of human keratinocytes, a cell line relevant to tissue engineering. A possibility of simultaneously preventing the injury from intracellular ice formation and slow-freezing injury by introducing a macromolecular non-permeant polyethylene glycol 400 as a sole cryoprotectant with rapid freezing was recognized. Thermoanalytical and microstructural analysis of the potential cryoprotective mixture has been performed to test its efficacy in preventing cell cryoinjury mechanisms. The post-thaw cell recovery indicated successful cryopreservation with a similar recovery to the standard slow-freezing protocol with permeant dimethyl sulfoxide. The novel approach represents an alternative cryopreservation strategy that avoids intracellular cryoprotectant toxicity and offers a simple freezing procedure (plunging into liquid nitrogen) and a more practical cryoprotectant wash-out after the thawing. The cryopreservation protocol also brings up new possibilities for applying macromolecular additives as novel cryoprotectants.

© 2023 Elsevier B.V. All rights reserved.

1. Introduction

Keratinocytes are conventionally cryopreserved by the standard slow-freezing procedure (1 °C/min) with 5 or 10 vol% dimethyl sulfoxide (DMSO) in a cell freezing medium. [1–4] Although skin and epithelial constructs were successfully cryopreserved by vitrification, [5,6] increase in cooling rate during cryopreservation of keratinocytes in suspension or monolayer led to a loss of cell viability when DMSO was applied as a cryoprotectant. [2,7] Cryopreservation, whether the conventional slow-freezing method or vitrification, aims primarily to prevent detrimental intracellular ice formation. The slow freezing approach avoids intracellular ice formation by allowing cell dehydration induced by freeze-concentration of dissolved salts in extracellular fluid. [8] However, the avoidance of intracellular ice formation is not sufficient for cell survival, and the presence of cryoprotective agents is required. Cry-

oprotectants are thought to prevent the slow-freezing injury caused by physicochemical changes of freeze-concentrated cell medium and associated cell exposure to elevated salt concentrations and cell dehydration. [9] The intracellular ice formation and slow freezing injury are conceptualized as two opposing mechanisms of cryoinjury acting at different applied cooling rates during the freezing of cells. [10] Although the mechanism of slow freezing (or “solution effects”) injury is not fully understood, it was found to be proportional to the duration of exposure to a freeze-concentrated solution, [11,12] suggesting the possibility of reducing the slow-freezing injury by minimizing the time of exposure to freeze-concentrated salts. In contrast to slow freezing cryopreservation protocols, vitrification avoids intracellular ice formation by introducing permeant cryoprotectants at high concentrations (~40 %), inducing a formation of an ice-free amorphous intracellular solution without the need for cell dehydration. Besides the intracellular ice formation and “solution effects” injury, there is also evidence of adverse effects of extracellular ice on cell survival. [13,14] In addition to the water/ice phase transition, the

* Corresponding author.

E-mail address: ivan.klbik@savba.sk (I. Klbik).

eutectic crystallization of sodium chloride and other salts naturally present in the cell (freezing) media was also associated with direct cell injury and significant loss of cell viability.[15] It was shown that eutectic crystallization of NaCl is avoided by even relatively low concentrations of dimethyl sulfoxide (≥ 2 vol%) [16] correlating with the strongly concentration-dependent cryoprotective action of DMSO in human stem cells cryopreservation, [17–20] suggesting that inhibition of eutectic crystallization is an aspect of the cryoprotective mechanism provided by DMSO and similar cryoprotectants.

Both slow-freezing and vitrification protocols have certain practical drawbacks. Both approaches typically rely on permeant cryoprotectants, which enter cell cytoplasm and might be toxic. [21,22] A sufficiently high concentration of a cryoprotectant is needed to induce cryoprotection. Removal of the cryoprotectant following the thawing of cryopreserved cells might be desired, requiring a timely post-thaw wash-off, which may cause additional cell injury. [23] Another drawback of the standard slow-freezing protocol is the requirement of a controlled-rate freezer or equipment controlling the cooling rate during the freezing.

Based on the knowledge of cell cryoinjury, an effort was made to design a cryopreservation protocol for HaCaT cells that would rely on a simple freezing method, avoid intracellular cryoprotectant toxicity and allow an easier cryoprotectant post-thaw wash-off. The possibility of simultaneously preventing intracellular ice formation and slow freezing injury was recognized by considering the effect of pre-freeze-induced cell dehydration by non-permeant cryoprotectants upon cells before freezing. Therefore, this study aims to design a novel protocol based on pre-freeze cell dehydration and to test its efficacy in HaCaT cell cryopreservation. The HaCaT cell line (Fig. 1) represents a model cell line sensitive to freezing-induced injury and is also of interest to tissue engineering research. [24].

2. Cryopreservation protocol design

Polyethylene glycol 400 (PEG 400) was chosen as a non-permeant cryoprotectant for HaCaT cell cryopreservation. This choice had a certain arbitrariness, as many other non-permeant macromolecular cryoprotectants would have also fulfilled the purpose. The choice of PEG 400 was motivated by its low toxicity, [25–27] availability, and successful application in the cryopreservation of other cells or cell structures in the past. [28,29] There are many PEGs with various lengths of the PEG molecule of different molecular weights. Before selecting a specific PEG, phase diagrams of binary water-polyethylene glycol mixtures were examined. It was found that PEGs induce the freezing point depression effect,

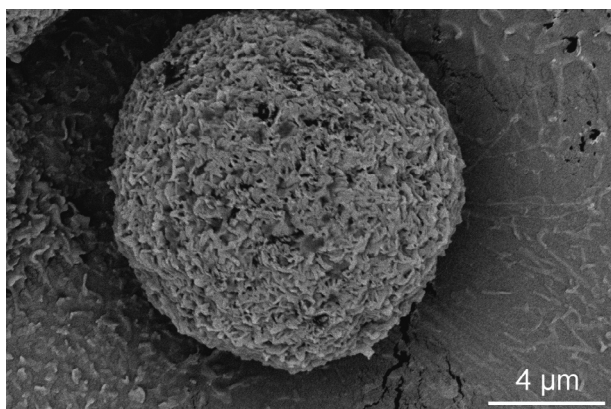


Fig. 1. A human keratinocyte as seen by scanning electron microscope.

reduce ice formation and that PEGs with higher molecular weights are subject to eutectic crystallization, while PEGs with lower molecular weights are not. [30] Since eutectic crystallization is considered a mechanism of cryoinjury, variants not exhibiting this kind of phase transformation were preferred. Note that this requirement might be unnecessary as, for example, DMSO, an effective cryoprotectant, is subject to eutectic crystallization in binary water-DMSO mixtures,[31] but in ternary mixtures with salts at comparable concentration, neither does DMSO nor salts crystallize eutectically.[16] Nevertheless, the complete absence of the eutectic reaction is beneficial. Since ethylene glycol – a monomeric unit of PEGs – is a cryoprotectant penetrating cell plasma membrane, to minimize the chance of permeation into the cell cytoplasm, a PEG with the highest possible molecular weight with no signs of eutectic crystallization - PEG 400, which has been considered plasma membrane impermeable, [32] was chosen. An indirect proof of its non-permeant nature might be given by the osmotic response of HaCaT cells assessed by optical microscopy, which revealed that cells suspended in phosphate-buffered saline (PBS) with 10 wt% PEG 400 shrank within 30 s and remained unchanged during 5-minute-long period (Fig. 2) – conditions representing the equilibration step preceding the freezing of cells (see Methods section).

To prevent cell cryoinjury and loss of cell viability during cryopreservation, the concentration of the PEG 400 in the cell freezing medium needs to be high enough to 1) prevent the eutectic crystallization of salts, 2) adequately limit the ice formation, and 3) induce significant cell dehydration before the freezing while not imposing too high hyperosmotic stress. Considering the cryoinjury caused by the eutectic crystallization of salts, it is beneficial to set the composition of the cell freezing medium so that any eutectic crystallization during freezing or thawing is avoided. Based on the study of the DMSO effect on the eutectic crystallization of sodium chloride,[16] a concentration-dependent inhibitory effect of PEG 400 upon the eutectic crystallization of salts might be expected. It was found that the eutectic crystallization of NaCl was gradually suppressed by increasing the DMSO concentration, and it was fully suppressed when a DMSO/NaCl concentration ratio equivalent to a ternary eutectic point was reached. It was argued that at such composition, crystalline phases (including pure NaCl) are thermodynamically favored that are more difficult to precipitate. The critical DMSO concentration needed to suppress the eutectic crystallization entirely was 2 vol% (in isotonic NaCl solution), equivalent to about 0.28 osmolal concentration of DMSO. Extrapolating the knowledge on the inhibitory effect of DMSO, with no assumption of any specific interaction between the PEG 400 and salts, the osmotic concentration of PEG 400 should be higher than ~ 0.28 Osm to suppress the eutectic crystallization of salts entirely. Nevertheless, it should be tested experimentally since non-ideal behavior might happen, which is difficult to predict.

The second requirement of sufficient reduction of ice formation is based on the work of Mazur and Cole,[13] who studied the effect of unfrozen fraction (an ice-free portion of freezing mixture) on the viability of red blood cells. The authors ascribed the detrimental impact of a too-low unfrozen fraction (< 0.15) to adverse interactions between extracellular ice and cells. Although some authors preferred another explanation considering the cell volume changes to be detrimental,[33] studies were published later to support the idea of cryoinjury imposed by extracellular ice formation.[14,34–38].

An insight into finding the optimal PEG 400 concentration, and thus the tonicity of the cryoprotective mixture, might be gained by considering the effect of hypertonic stress on HaCaT cells. HaCaT cells tolerated the hypertonic stress up to 0.5 Osm well, while an injury developed at 0.6 Osm tonicity of the bathing solution. [39]

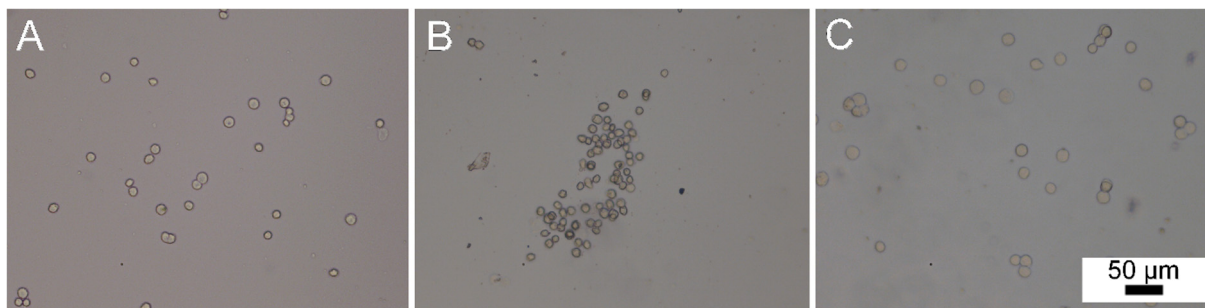


Fig. 2. Effect of cell medium osmolality on cell size: HaCaT cells suspended in isotonic PBS solution (A), a hypertonic solution containing PBS with 10 wt% PEG 400 (B), and a hypotonic solution prepared by 1:1 dilution of PBS and distilled water (C). The middle picture shows the dehydrating effect of non-permeant PEG 400 on HaCaT cells. The hypotonic solution is given just for comparison purposes. All pictures were obtained by optical microscope (transmitted light).

The cell medium must be hypertonic to apply the pre-freeze-induced cell dehydration cryopreservation protocol successfully. From the perspective of minimizing the intracellular ice formation, the PEG concentration could be set high enough that practically all osmotically active water would leave the cell and crystallize extracellularly. However, those levels of hypertonicity would be too high and could produce stress and cell injury. Therefore, to limit the hypertonic stress, the cryoprotective mixture's osmotic concentration should not exceed ~ 0.6 Osm. This led to the decision to add the PEG 400 at 10 wt% concentration to the cell freezing medium with resulting osmolality of about 0.66 Osm (assuming the additivity of PBS osmolality (0.3 Osm) and osmolality of PEG 400 in water – 0.36 Osm [40]). The level of cell dehydration developed by introducing the PEG 400 into the isotonic PBS solution was estimated by using the Boyle–van't Hoff relation, which states the following relation for the relative volume of osmotically active cell water V_w (normalized to isotonic volume):

$$V_w = \frac{m_0}{m} \quad (1)$$

Where m_0 and m are the isotonic osmolality (0.3 Osm) and the actual osmolality of the cryoprotective mixture, respectively. Based on this calculation, assuming ideal cell osmotic behavior, the loss of osmotically active intracellular water might be estimated to be 55%. Such loss of intracellular water could considerably reduce the injury imposed by intracellular ice formation and enable the application of a high cooling rate during subsequent freezing. Simultaneously, the slow freezing injury should be minimized by the high cooling rate and limited duration of exposure to freeze-concentrated salts and cryoprotectants. In addition, the reduced size of extracellular ice crystals associated with a higher cooling rate applied during freezing could also benefit the viability of cryopreserved cells. [41] Therefore, this protocol could successfully cryopreserve HaCaT and other cells. However, the absence of the cryoprotectant in the cell cytoplasm might be problematic. It is often assumed that cryoprotectants must be present in the cell cytoplasm to suppress the “solution effects” injury and enable successful cryopreservation cells. [42] However, this might not necessarily be the case, as, for example, T lymphocytes were protected by non-permeant trehalose against the “solution effects” injury. [43] A possibility to successfully cryopreserve keratinocytes without permeant cryoprotectant was already demonstrated in a study by Pasch et al., in which hydroxyethyl starch was used as a non-permeant cryoprotectant in combination with relatively slow freezing (3 °C/min). [44] In addition, the injury should be minimized by the high cooling rate and associated limited exposure to the concentrated solution.

To test the efficacy of the PEG 400 to suppress the recognized forms of cryoinjury, a thermoanalytical and microstructural analysis of the 10 wt% PEG 400-based cryoprotective mixture was performed and compared to the standardly used 10 vol% DMSO. The

proposed cryopreservation protocol was also tested in the cryopreservation of primary HaCaT cells, and its efficacy was compared to the standard slow freezing (1 °C/min) cryopreservation protocol with 10 vol% DMSO.

3. Methods

3.1. Cryopreservation procedure and cell survival test

Human keratinocytes (HaCaT cell line) were cultured in Dulbecco's modified Eagle's medium at 37 °C, 5% CO₂, and 72% humidity. Cells suspended in a culture medium were centrifuged (3 min, 1500 rev/min) and resuspended in isotonic phosphate-buffered saline (137 mM NaCl, 2.7 mM KCl, 8.54 mM Na₂HPO₄, 1.46 mM KH₂PO₄, pH 7.4). The addition of PEG 400 was performed by 1:1 dilution of 20 wt% PEG 400 in PBS, resulting in approximately 10 % PEG 400 in PBS with a cell concentration of about 10⁶/ml. Cells were equilibrated for 5 min at room temperature and then frozen by plunging the 1.8 ml vials into liquid nitrogen and stored for 2 h. The cooling rate induced by a plunge into liquid nitrogen was not measured in this study. It is expected to be in the range of 100 – 200 °C/min. [45] The thawing procedure was performed in a 50 °C water bath. Cell preservation rate was assessed by the trypan blue exclusion method 30 min after the completion of thawing. To evaluate the efficacy of the designed protocol, HaCaT cells were also cryopreserved with 10 vol% DMSO in the cell freezing medium by the standard slow freezing protocol (1 °C/min) to –80 °C and stored in the vapor phase of liquid nitrogen. Thawing was performed in a 50 °C water bath. The shown results of the cryopreservation are given by the range of obtained cell preservation rates (normalized to the initial number of cells) of two independent experiments.

3.2. Differential scanning calorimetry

The studied cryoprotective mixtures containing cells or cell-free were subjected to DSC analysis, allowing phase diagram determination and quantification of phase transitions. DSC analysis was performed with a power-compensated calorimeter Perkin-Elmer 8500DSC equipped with an Intracooler device (–73 °C) for measurements in a temperature range of –70 to 15 °C. The applied cooling and heating rates were 5 °C/min. The studied mixtures (~ 20 mg) were encapsulated in aluminum pans, and nitrogen with a flow rate of 20 ml/min was used as a dynamic atmosphere. Each DSC measurement was repeated at least once: two measurements of cell-containing solutions and three measurements of cell-free freezing media were performed. The phase transition temperatures and enthalpies are given by a mean value and standard deviation, or range of obtained values in the case of cell-containing solutions.

3.3. Positron annihilation lifetime spectroscopy

The PALS technique represents a nuclear physics experimental method that exploits the formation of positron–electron pair (positronium) to probe the microstructure of various materials. The lifetime of positronium is sensitive to structural changes and phase transformation, [46,47] allowing for its application in phase behavior studies of water, [48,49] aqueous mixtures, [20] organics, [50] metals [51] or polymers. [52] It represents a complementary method to calorimetry and optical cryomicroscopy as it allows the detection of phase transformations, which might be undetectable by these methods. ^{22}Na was used as a positron source. The studied cell-free cryoprotective mixtures were injected into aluminum sample chambers, which surrounded the positron source (sandwich geometry). The positron lifetime spectra collected with scintillation detectors Scionix 25.4B12/2M–Q–BAF–X–N were corrected to the contribution of positron source and Kapton foil used in the sample chambers. The width of the prompt response function was determined by measuring a defect-free silicon sample and was determined to be 300 ps (full width in half of the resolution function maximum). The lifetime spectra were analyzed and deconvoluted by freely available LT Polymers software [53] with three-component fit accounting for direct positron–electron annihilation, *para*-positronium, and *ortho*-positronium formation. The longest lifetime component is attributed to the formation of *o*-Ps, which annihilates by pick-off annihilation with surrounding matter and thus reflects the local microstructure of the studied material. The mean lifetimes of *o*-Ps in the studied cell-free solutions with a standard deviation were obtained during one-hour isothermal measurements at selected temperatures in the range of -170 to 30 °C. A closed-cycle Helium refrigerator JANIS CCS-450 System with temperature stability ± 0.2 °C was used for low-temperature measurements.

3.4. Raman micro-spectroscopy

A confocal microscope Olympus BX-41 equipped with LabRAM-HR 800 spectrometer was used to study frozen mixtures' microstructure and obtain their Raman spectra. A laser with a wavelength of 532 nm was used as an illumination source. The signal was dispersed using a diffraction grating with 600 grooves per mm onto a cooled CCD (charge-coupled device) detector. The resolution of the system was better than 6 cm^{-1} , and the spectral accuracy was verified on Teflon strips. Raman spectra were collected in the range of Raman shift from 200 to 4000 cm^{-1} . Low-temperature measurements were allowed by a liquid nitrogen cooling accessory (Linkam THM-600). For the study of ice microstructure, a drop of cell-free solution was put on a microscope glass and covered with cover glass, forming a thin liquid layer. For the Raman spectroscopy, an uncovered drop of solution was studied. A cooling rate of 100 °C/min was applied to simulate conditions experienced by cells in the designed cryopreservation protocol based on PEG 400. The ice microstructure was compared to the cryopreservation standard 10 vol% DMSO cooled at 10 °C/min.

4. Results and discussion

4.1. Effect of the PEG 400 on the phase behavior of cell freezing medium

Cell-free and cell-containing cryoprotective mixtures were studied by differential scanning calorimetry. These experiments aimed to show how the PEG 400 affects the ice formation, eutectic crystallization of salts, and how the presence of cells affects the

solid–liquid phase transformations of the cell medium. DSC thermogram showing the phase behavior of these cell suspensions is shown in Fig. 3 (top). In PBS (black curve), ice and eutectic crystallization occurred only after some supercooling. The eutectic crystallization was completed in (roughly) two steps, as indicated by two distinctive exothermic peaks at about -30 °C and -40 °C. [16] The two-step nature of the eutectic phase transformation is also observed during the melting (inset of Fig. 3 - top) – the dominant peak (-22 °C) is clearly associated with the melting of NaCl dihydrate and ice as comparison with binary NaCl–water mixture suggests. The minor peak at a slightly lower temperature (-23 °C) must be caused by the presence of phosphates and/or potassium. Its temperature agrees with the ternary eutectic point of the water–NaCl–KCl mixture (-22.9 °C).[54] Various eutectic phases might form considering the multi-component nature of PBS solution. Eutectic phases based on Na_2HPO_4 , KH_2PO_4 , NaH_2PO_4 , K_2HPO_4 were recorded between -16.7 °C and -0.5 °C.[55] These might be difficult to detect, considering their minor contribution to the salt content and the dominance of the DSC signal associated with ice melting in that temperature range. Comparing the thermograms of PBS and binary aqueous NaCl solution (Fig. 3 - bottom), it is evident that the eutectic crystallization is more complex in the case of PBS. Exothermic peaks at about -30 °C are absent in the binary NaCl–water mixture, supporting the differential effect of KCl and/or phosphates. The presence of HaCaT cells (at a number of $10^6/\text{ml}$) did not significantly affect the phase

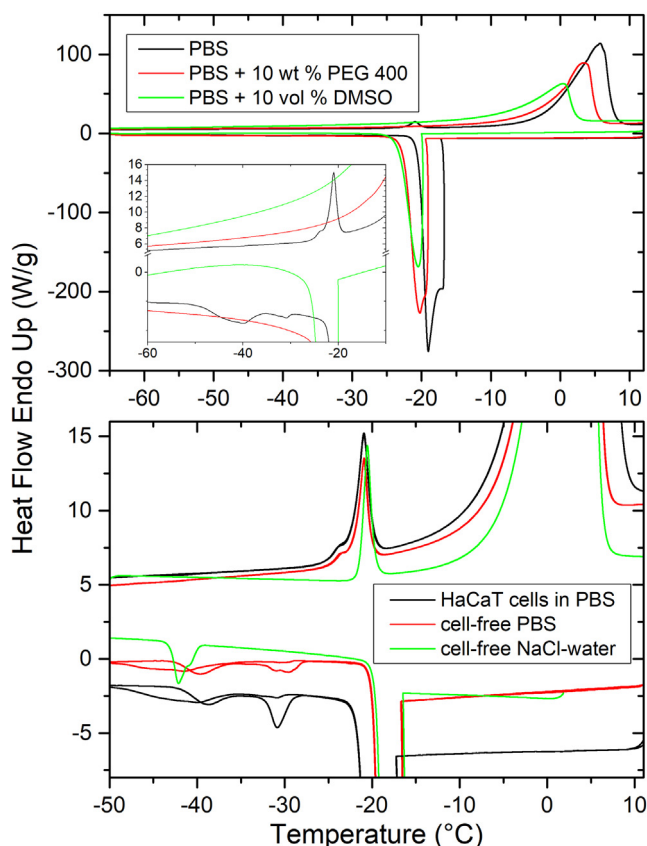


Fig. 3. Heating and cooling DSC thermograms: Top: Cell-containing cell freezing media - the picture shows the suppressing effect of DMSO and PEG 400 on ice and eutectic formation (inset). Bottom: eutectic melting and crystallization in cell-free, cell-containing PBS and cell-free binary 0.9 wt% NaCl in water – thermograms show the insignificant effect of HaCaT cells on phase transformation of cell medium and differential effect of the phosphates and potassium on the eutectic phase transformation.

behavior of the cell medium; only negligible differences in the enthalpy of fusion of ice were detected (data not shown).

Importantly, DSC analysis revealed that the addition of 10 wt% PEG 400 (red curve in Fig. 3 - top) to the PBS cell medium inhibits the eutectic salt crystallization associated with the solidification process of isotonic phosphate-buffered saline solution. During the freezing and thawing, no thermic reaction was detected that could be ascribed to a first-order eutectic phase transformation. Therefore, the 10 wt% PEG 400 offers protection against the injury imposed by the eutectic crystallization of salts, similar to the cryopreservation standard 10 vol% DMSO, which also prevents the eutectic salt crystallization. Note that in the case of DMSO, a minor deviation of the heat flow curve was detected at about $-18\text{ }^{\circ}\text{C}$ suggesting a trace eutectic formation.

For comparison of results and the effect of PEG 400, DSC analysis of cell-free binary aqueous PEG 400 mixture (10 wt%) was performed. DSC thermograms show the depression of the ice freezing point induced by PEG 400. No signs of eutectic crystallization in binary aqueous PEG 400 mixture were recorded (Fig. 4), consistently with previously published work. [30] It has been suggested that low-molecular-weight PEGs, including PEG 400, cannot reach an ideal crystalline state due to the insufficient chain length to form an ordered helix structure in crystal and that interaction between water and PEG 400 is not strong enough to form intermediate crystalline structures (hydrates). The absence of eutectic crystallization in a binary water-PEG 400 mixture is a good prerequisite for the cryoprotective potential of PEG 400, minimizing the overall chance of eutectic crystallization in actual cell-freezing media. It might be interesting to compare the binary mixture with the cell freezing medium, including PBS (Fig. 4). The ice melting temperature and ice melting enthalpy is lower in the case of PBS solution supplemented with 10 wt% PEG 400. This is an expected result when no preferential interaction between salts and PEG 400 is assumed. The depressing effect of salts and PEG 400 on the ice melting temperature is roughly additive.

The calorimetric analysis also revealed that the heat absorbed during the melting of ice in 10 wt% PEG 400 in isotonic PBS is equal to about 246 J/g (normalized to the weight of the solution), indicating a considerably reduced amount of ice in the frozen mixture (heat of fusion of pure ice is 333.5 J/g). From the perspective of the “unfrozen fraction” hypothesis, [13] it is useful to quantify the amount of ice or amount of unfrozen fraction of water, which might be done by comparing the ice enthalpy of fusion in the mix-

ture (normalized to the weight of the water in the mixture) to the enthalpy of fusion of pure ice:

$$U = \frac{\Delta H_{\text{mix}}}{\Delta H_{\text{ice}}} \quad (2)$$

The results of this quantification are listed in Table 1. The lowest unfrozen fraction of water characterizes the cryoprotectant-free PBS solution. Although there is an unfrozen fraction of water above the eutectic point, it vanishes upon eutectic crystallization (see also Fig. 5). The addition of 10 wt% PEG 400 formed an unfrozen fraction of water of 0.172, which remains liquid (amorphous) during the complete solidification and melting process. Compared to 10 vol% DMSO, the PEG-based mixture offers weaker protection against ice formation. However, the amount of ice in the PEG 400-based mixture is similar to 5 vol% DMSO ($\sim 245.5\text{ J/g}$), sufficient for successful HaCaT cryopreservation, [1] therefore, it is concluded that 10 wt% PEG 400 offers adequate protection against the cryoinjury imposed by extracellular ice. The suppressing effect of PEG 400 on ice and eutectic formation might be ascribed to the non-specific effect on the thermodynamics of mixtures when the chemical potential of water is depressed, shifting the solid-liquid equilibrium to a lower temperature – applying both to the ice and eutectic melting point. The benefit specific to PEG 400 is that it does not precipitate out of the freeze-concentrated solution. Therefore, a certain fraction of the freezing mixture remains ice-free during the whole solidification and melting process, protecting cells primarily against extracellular ice.

4.2. Ice microstructure analysis

Polycrystalline ice is typically formed during the freezing of water and aqueous mixtures. The overall microstructure comprises many individual ice crystals of various sizes and shapes (Fig. 5). Water-soluble additives in aqueous solutions are subject to the freeze-concentration process as liquid water leaves the liquid solution while transforming to ice. The liquid freeze-concentrated liquid separates ice crystals (see the top of Fig. 5), and biological cells (not in the picture) are rejected from the ice into the freeze-concentrated solution. [56] The concentrations of the dissolved substances rise during freeze-concentration and eventually reach the eutectic concentration at which a eutectic reaction occurs, representing a threat to cell viability. It has been shown that crystallized NaCl dihydrate directly surrounds the cell plasma membrane [57,58] and that eutectic NaCl crystallization causes a direct cell injury compromising post-thaw cell recovery. [15] Cell (freezing) media naturally contain salt, mimicking the composition of extracellular fluid. The phosphate-buffered saline solution used in this study contains NaCl, KCl, and phosphates which buffer the pH of the solution. All these substances are subject to eutectic crystallization during the solidification in a mixture with water. [55,59–61] The eutectic crystallization of these substances and the associated change of optical appearance is shown in Fig. 5 (note the difference between the top and bottom picture).

The effect of PEG 400 and standard cryoprotectant DMSO on ice microstructure was examined by an optical cryo-microscope. A comparison of the microstructures formed during the solidification of PEG 400 and DMSO-based cryoprotective mixtures shows the differential effect of the applied cooling rate (Fig. 6). While the PEG 400 containing the mixture was frozen at $100\text{ }^{\circ}\text{C/min}$, the mixture with DMSO was frozen at $10\text{ }^{\circ}\text{C/min}$. As expected, the higher cooling rate resulted in the formation of a higher number of ice crystals of smaller size, while the slow cooling rate had the opposite effect. The smaller size of extracellular ice crystals might be beneficial, as was suggested in a study by Kratochvílová et al. [41] There was also no darkening of the space between ice crystals, and ice appeared to be the only crystalline phase formed during

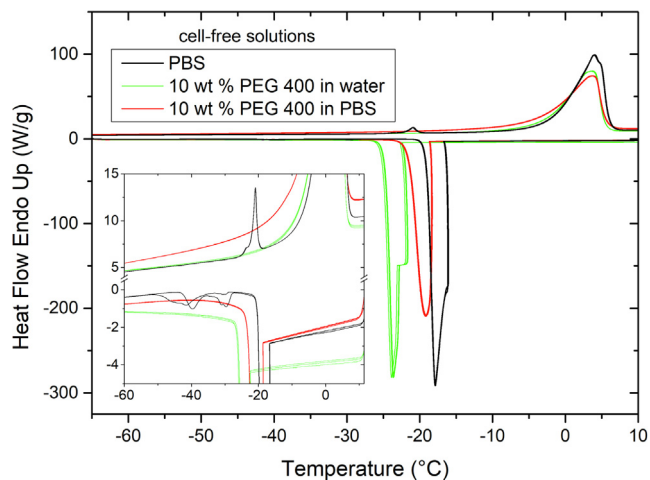


Fig. 4. Heating and cooling DSC thermograms showing the phase behavior of binary aqueous PEG 400 mixture compared to PBS and PBS + 10 wt% PEG 400. For phase transition characteristics, see Table 1.

Table 1

Phase transitions characteristics of cell-free solutions. Enthalpy is normalized to the weight of the whole cell-free solution. The unfrozen fraction (of water) is normalized only to the water weight present in the solution. The results are given by a mean value and standard deviation of three measurements.

| Cell freezing medium | Ice melting temperature (°C) | Ice enthalpy (J/g) | Eutectic temperature (°C) | Eutectic enthalpy (J/g) | Unfrozen fraction |
|------------------------|------------------------------|--------------------|---------------------------|-------------------------|-------------------|
| PBS | -0.82 ± 0.13 | 293.98 ± 2.30 | -22.16 ± 0.13 | 7.23 ± 0.04 | 0 |
| PBS + 10 vol% DMSO | -8.88 ± 0.05 | 208.22 ± 2.51 | ~ -18 | trace | 0.291 ± 0.009 |
| PBS + 10 wt% PEG 400 | -3.62 ± 0.01 | 246.07 ± 2.07 | - | 0 | 0.172 ± 0.007 |
| 10 wt% PEG 400 + water | -2.55 ± 0.07 | 257.63 ± 2.43 | - | 0 | 0.133 ± 0.008 |

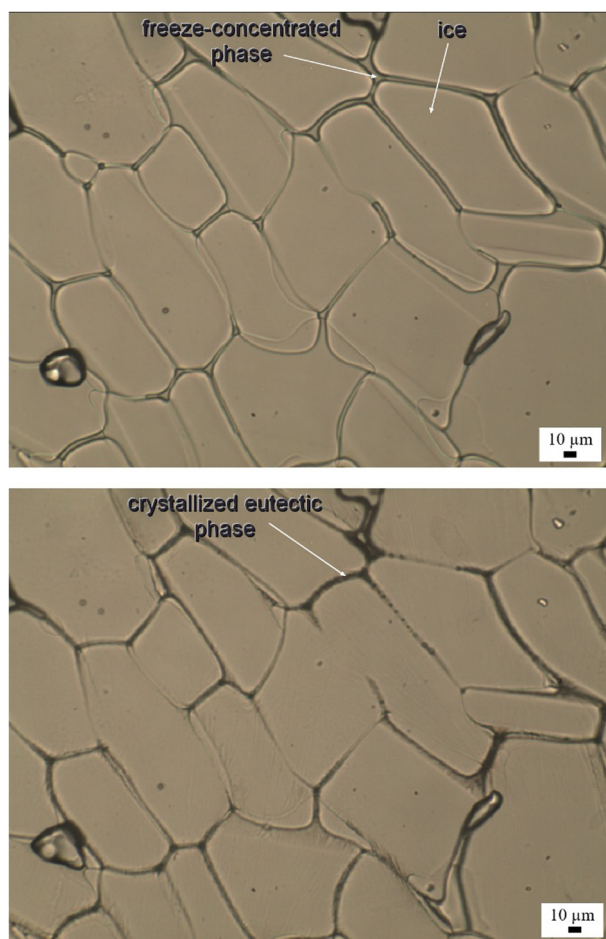


Fig. 5. Ice microstructure in cell-free PBS medium frozen at 10 °C/min. The pictures are obtained by an optical microscope operated in the transmitted light mode. Top: -20 °C, bottom: -45 °C. Besides the size and shape of the ice crystals, the bottom picture shows completed eutectic crystallization, which visually occurred at about -37 °C and was associated with the darkened optical appearance of space between the individual ice crystals.

the freeze–thaw cycle. The emphasis was also put on the temperature stability of the formed ice microstructure of the PEG 400-based cryoprotective mixture. The cryo-microscopic analysis revealed high stability of the formed microstructure, which remained stable even during slow thawing (step-wise heating from -125 °C to 0 °C at 10 °C/min with isothermal holdings (~ 30 s) at every 10 °C) when no apparent changes to the microstructure occurred. Note that ice microstructure formed in a slowly frozen 10% DMSO-containing medium also showed high stability.

4.3. Raman spectroscopy

Raman spectroscopy analysis was performed alongside the optical microscopy measurements to further support the presence of an amorphous freeze-concentrated phase. Raman spectra of

cryoprotectant-free, PEG-, and DMSO-based mixtures in the liquid state are characterized by broad water OH-stretching peaks in the range of about $3000 - 3700$ cm^{-1} (Fig. 7). In addition, the cryoprotective mixture containing DMSO shows intense Raman peaks associated with vibrations of DMSO molecules at 678 , 713 , 2926 , 3013 cm^{-1} , which might be attributed, based on the Raman spectrum of pure DMSO, [62] to C-S symmetric stretch, C-S asymmetric stretch, C-H symmetric stretch, and C-H degenerate stretch, respectively. The Raman spectrum also showed additional less pronounced peaks in the range of $300 - 400$ cm^{-1} (C-S-C and C-S-O bends), 952 cm^{-1} (CH_3 rocking), 1015 cm^{-1} (SO stretch), and a peak at 1418 cm^{-1} , which is attributed to CH_3 degenerate deformation. Note that most vibrations are shifted by about 10 cm^{-1} compared to pure DMSO. Exceptions are C-S-C bend at about 305 cm^{-1} , CH_3 rocking at 952 cm^{-1} , and CH_3 degenerate deformation (1418 cm^{-1}), which are almost unaffected, and SO stretch (1013 cm^{-1}) being the most shifted vibration (1042 cm^{-1} in pure DMSO). Especially the SO stretch offers the possibility to quantify the structure of DMSO in mixtures with water since it changes with the DMSO concentration in the mixture. [63] The position of the Raman peak associated with the SO stretch was 1013 cm^{-1} in the liquid state (25 °C – Fig. 7) and 1009 cm^{-1} in the frozen state (-150 °C – Fig. 8), implying the hydrated structure of DMSO and the absence of crystalline DMSO in the frozen state. There was also no splicing of the peak associated with C-H symmetric stretching (2926 cm^{-1}), which might be expected to occur in the pure crystalline DMSO. [64] Simultaneously, there were no signs of NaCl dihydrate formation, which is the dominant crystalline eutectic phase besides ice in the cryoprotectant-free PBS and is associated with Raman peaks at 3422 and 3539 cm^{-1} . [65]

The Raman spectrum of the PEG 400-based cryoprotective mixture (Figs. 7 and 8) is characterized by a pronounced convolution in the range of $2800 - 3000$ cm^{-1} due to CH stretching modes and a series of less intense Raman peaks in the range of $800 - 1500$ cm^{-1} : CH_2 rocking and twisting (808 cm^{-1}), CO stretching (with a contribution of CH_2 rocking and CC stretching) (837 , 848 , 886 cm^{-1} , and $1040 - 1140$ cm^{-1}), CH_2 twisting ($1240 - 1280$ cm^{-1}), and CH_2 scissoring ($1440 - 1480$ cm^{-1}). [66,67] Comparing the Raman spectra of pure PEG 400 and hydrated PEG 400, [68] it might be concluded that the convolution of Raman peaks in the range of $2800 - 3000$ cm^{-1} (Fig. 8, -125 °C) is associated with hydrated PEG 400 in an amorphous state. The convolution's first major peak (symmetrical CH stretching) in the pure PEG 400 is located at 2879 cm^{-1} . [68] It shifts and approaches 2891 cm^{-1} with increasing water content. In the PEG-based cryoprotective mixture studied in this work, the location of the first peak is 2891 cm^{-1} at 25 °C and 2893 cm^{-1} at -125 °C, supporting the presence of hydrated structure in the frozen state. In addition, the overall shape and relative intensities of individual peaks of the $2800 - 3000$ cm^{-1} convolution resemble more the hydrated state than pure PEG 400. [68] Similar to the DMSO-based cryoprotective mixture, no signs of NaCl dihydrate formation were detected. Overall, these results support the DSC analysis and considerations of optical appearance, which indicated the formation of an amorphous freeze-concentrated phase during the freezing of PBS with 10 wt % PEG 400.

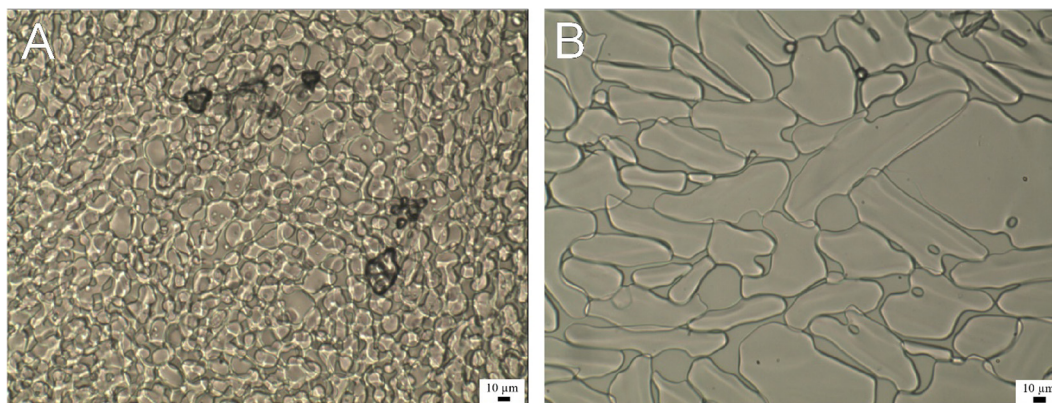


Fig. 6. Ice microstructures obtained by optical microscope operated in transmitted light mode. A) PBS with 10 wt% PEG 400 cryoprotective mixture frozen at 100 °C/min cooling rate. B) PBS with 10 vol% DMSO cryoprotective mixture frozen at 10 °C/min. Note that the darker spots on micrographs are associated with air bubbles, not any crystalline phase.

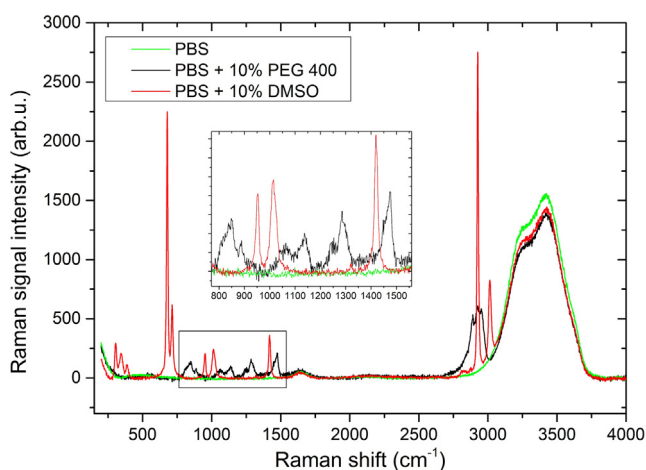


Fig. 7. Raman spectra of PBS, PBS with 10 wt% PEG 400, and PBS with 10 vol% DMSO obtained at 25 °C.

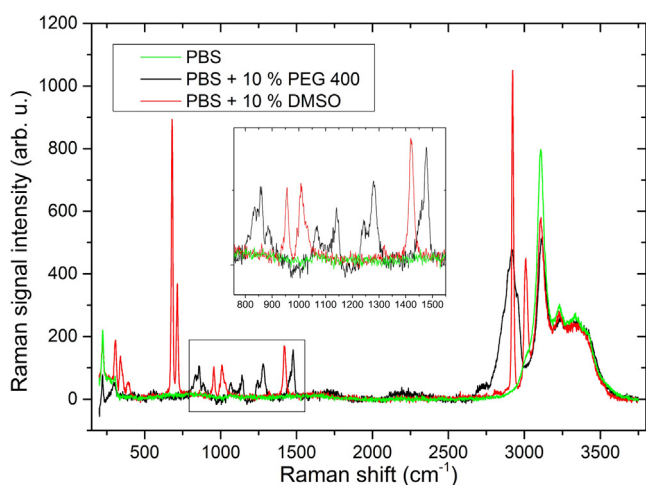


Fig. 8. Raman spectra of PBS (-150 °C), PBS with 10 wt% PEG 400 (-125 °C), and PBS with 10 vol% DMSO (-150 °C) in the frozen state.

4.4. Local microstructure characterization

Positron annihilation lifetime spectroscopy (PALS) was employed to verify the temperature stability of the formed ice

microstructure and amorphous freeze-concentrated phase against any phase transformations that might not be detected by calorimetry or optical microscopy. Our research group has previously applied this technique to study phase behavior and microstructural free-volume properties of aqueous solutions relevant to cryobiology. The ability to detect and observe eutectic phase transformations and differentiate between crystalline and amorphous structures was shown for water-DMSO,[20,69] water-NaCl, and water-NaCl-DMSO mixtures,[16] qualifying the method for application in this study.

The temperature behavior of *ortho*-positronium (*o*-Ps) lifetimes exhibited a significant change between -20 °C and 0 °C during the melting and solidification of the cryoprotective mixture containing 10 wt% PEG 400 (Fig. 9 - top). This behavior is associated with ice melting and crystallization, representing a dominant phase in the mixture at a 10 wt% concentration of PEG 400. This *o*-Ps lifetime behavior is similar to pure water [20,70] and differs only in the temperature range of the phase transformation, as expected by considering the freezing point depression effect. Besides the supercooling of water and associated ice formation between -15 °C and -20 °C, there is no considerable hysteresis between the *o*-Ps lifetimes obtained during freezing and thawing of the PEG-based mixture, indicating the formation of stable local microstructure with no apparent first-order phase transformations below -30 °C. There were no signs of any cold crystallization, which might occur during the thawing of the frozen aqueous mixtures, as was detected in the DMSO-based mixtures with DMSO concentrations (<2 vol%) that were insufficient to suppress the eutectic crystallization entirely. [16] The PALS analysis also did not detect any phase transformation, which could be associated with the formation of NaCl dihydrate or any other eutectic crystalline phase. This outcome is consistent with the DSC analysis and other techniques, which revealed a complete avoidance of first-order eutectic phase transformation in the presence of 10 wt% PEG 400. Compared to cryoprotectant-free PBS solution, the PEG 400-based medium is characterized by globally higher *o*-Ps lifetimes through the whole temperature range of the heating measurements (Fig. 9 - bottom). The higher *o*-Ps lifetimes signify the presence of a liquid or an amorphous fraction in the mixture. In the temperature range between -60 and -20 °C, the presence of 10 vol% DMSO resulted in higher *o*-Ps lifetimes than the PEG 400-containing mixture. This result is consistent with the expected lower ice fraction in the frozen mixture containing DMSO (see the ice melting enthalpies in Table 1). However, the trend is reversed between -80 and -120 °C, possibly due to the difference in glass transition temperature between the two cryoprotective mixtures and different

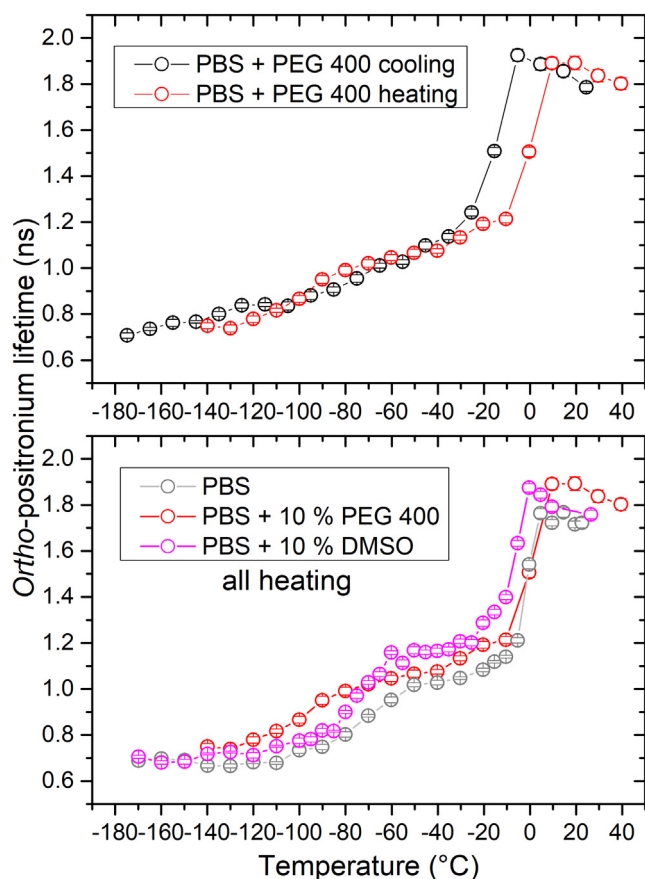


Fig. 9. Ortho-positronium lifetimes during freezing or thawing of the studied cell-free freezing media. Top: solidification and melting of PEG 400 mixture. Bottom: melting of cryoprotectant-free PBS, DMSO mixture, and PEG mixture. Ortho-positronium lifetimes are given by a mean value with standard deviation, which is of similar size as data points.

dynamic behavior during solidification, considering the polymeric nature of PEG 400.

Overall, the thermoanalytical and microstructural analysis revealed a successful avoidance of eutectic crystallization, sufficient reduction of ice formed, and reduced ice crystal size with high stability of ice microstructure formed during rapid freezing of the 10 wt% PEG 400 mixture. Similar to the effect of DMSO on solid-liquid equilibria, [16] the PEG 400 seems to compete with NaCl and other salts for interactions with water in a freeze-concentrated liquid phase, thermodynamically suppressing the formation of NaCl dihydrate and other possible eutectic crystalline phases. This outcome qualifies the PEG-based cryoprotective mixture as a potential candidate for application in actual HaCaT cryopreservation.

4.5. HaCaT cryopreservation

A post-thaw cell survival assessment performed 30 min after the thawing procedure revealed 75–82% survival of HaCaT cells cryopreserved by rapid freezing with PEG 400 as a sole cryoprotectant (Fig. 10). The recovery of HaCaT cells was significantly enhanced compared to the cryoprotectant-free cell freezing medium containing only the PBS solution. This result supports the rationalization of the novel cryopreservation protocol, which minimizes the cryoinjury imposed by intracellular and extracellular ice formation, slow freezing injury, and eutectic crystallization. The recovery obtained by the rapid freezing with PEG 400 is compara-

ble to the conventional slow freezing (1 °C/min) with 10 % DMSO, which secured 80–85 % survival. Both approaches resulted in a loss of some cell preservation rate, suggesting the existence of either an additional mechanism of cell cryoinjury not considered in the design of the cryopreservation protocol or not fully minimized cryoinjury imposed by intracellular ice formation or “solution effects” injury. At conditions that cells face during the proposed cryopreservation protocol, intracellular ice formation cannot be completely ruled out—the osmolality of cell freezing medium containing the isotonic PBS and 10 wt% PEG 400 is about 0.66 Osm, representing a moderately hyperosmotic solution. As mentioned before, the PEG 400 concentration in the freezing medium could be perhaps increased since the 5-minute-long exposure of HaCaT cells to the PEG-containing cell freezing medium (at 23 °C) did not result in any significant loss of cell survival (data not shown), suggesting the possibility for an optimization of the protocol.

The novel HaCaT cryopreservation protocol represents an alternative to the standard slow freezing and vitrification. A 1 °C/min cooling rate is often applied to cryopreserve cells in slow freezing methods. Our approach shares more similarities with the vitrification method as both rely on a high cooling rate during freezing. However, in our approach, the 10 wt% concentration of PEG 400 is relatively low considering the vitrification standards. Another critical difference to vitrification methods lies in the non-permeant nature of PEG 400, which does not enter the cell cytoplasm. In contrast, the vitrification is often accomplished by introducing permeant cryoprotectants (such as DMSO, glycerol, and ethylene glycol) at a considerably higher concentration (~40 wt %). The pre-freeze-induced cell dehydration approach is more similar to the two-step freezing method, [71,72] usually relying on the passive (uncontrolled) freezing to an intermediate subzero temperature, such as –30 °C, followed by a direct plunge to liquid nitrogen. However, in the pre-freeze-induced cell dehydration cryopreservation protocol, the freezing is completed in one step. Compared to the two-step freezing method, it offers better protection against the “solution effects” injury, which might occur even during the short-term (~minutes) isothermal holding at the intermediate subzero temperature. We have found that an approach based on pre-dehydration was applied recently to cryopreserve red blood

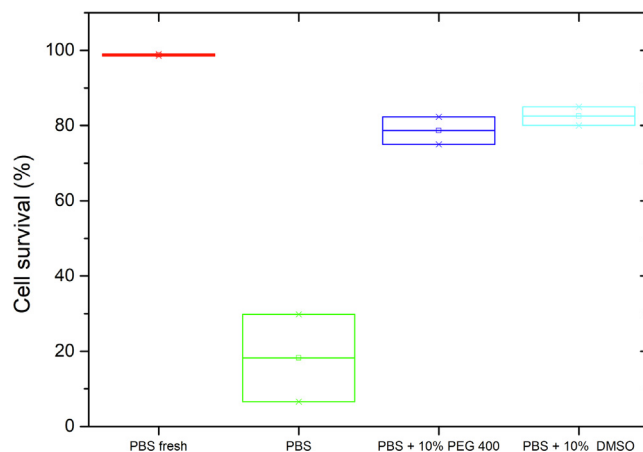


Fig. 10. Normalized absolute cell preservation rate estimated by trypan blue exclusion method. Results are given by a mean and range of obtained values. The first column, fresh cells, refers to not cryopreserved cells. Other columns refer to the post-thaw recovery of cryopreserved HaCaT cells in PBS alone, PBS with 10 wt% PEG 400 (both frozen by the plunge into liquid nitrogen), and PBS with 10 vol% DMSO frozen by conventional slow freezing protocol (1 °C/min). (For interpretation of the references to colour in this figure legend, the reader is referred to the web version of this article.)

cells, fibroblasts, and mesenchymal stem cells. [73] However, the ice seeding step was included making the freezing procedure a two-step process. The authors used another non-permeant cryoprotectant, trehalose. More recently, red blood cells, which are devoid of intracellular compartments, were cryopreserved with trehalose and without the ice seeding step. [74] Our results suggest that even more complex cell types with intracellular compartments may be cryopreserved by rapid freezing without high concentrations of permeant cryoprotectant. Successful application of different cryoprotectants in similar cryopreservation protocols supports the non-specific mode of cryoprotective action of these two cryoprotectants. Therefore, the application of other relatively non-toxic and non-permeant additives might also be expected to be successful in such cryopreservation protocol, bringing up new possibilities for the design of cryoprotective mixtures focusing on macromolecular substances, which might limit the toxicity associated with common permeant cryoprotectants.

5. Conclusions

A novel protocol for cryopreservation of human keratinocytes (HaCaT) was developed based on the current state of cryobiological knowledge. The protocol relied on non-permeant cryoprotectant polyethylene glycol 400 introduced at 10 wt% concentration as a sole cryoprotectant and a rapid freezing procedure accomplished by a direct plunge into liquid nitrogen. Compared to conventional cryopreservation methods, this protocol represents an alternative approach to slow freezing and vitrification. Based on the effect of PEG 400 on the solid–liquid phase transformation of cell freezing medium, the cryoprotective action of polyethylene glycol 400 was attributed to the ability to (1) moderately increase the osmolality of an extracellular solution, causing pre-freeze cell dehydration due to its non-permeant nature, (2) suppress the extracellular ice formation, and (3) inhibit the eutectic crystallization of salts. The suppressing effect of PEG 400 is ascribed to the non-specific effect on the thermodynamics of mixtures with the benefit of PEG 400 forming amorphous hydrated structures during solidification, minimizing the chance of formation of crystalline eutectic phases. The pre-freeze-induced loss of intracellular water allows for the application of rapid freezing protocol with minimized risk of detrimental intracellular ice formation. At the same time, the time-dependent slow-freezing injury is reduced due to the applied high cooling rate. The formation of smaller extracellular ice crystals associated with plunge freezing might also improve post-thaw recovery. The benefits of this protocol are the avoidance of intracellular cryoprotectant toxicity, easy-to-use freezing and thawing process, and a more practical procedure of PEG 400 wash-out after the thawing procedure. Considering the non-specific cryoprotective action of the PEG, the pre-freeze-induced cell dehydration approach brings up new possibilities for novel cryoprotectants based on macromolecular additives or other non-permeant agents without the need for permeant cryoprotectants that often introduce some toxicity.

CRedit authorship contribution statement

Ivan Klbik: Conceptualization, Validation, Formal analysis, Investigation, Writing – original draft, Writing – review & editing. **Katarína Čechová:** Methodology, Resources, Writing – review & editing. **Stanislava Milovská:** Resources, Investigation, Writing – review & editing. **Helena Švajdlenková:** Resources, Writing – review & editing. **Igor Maňko:** Resources, Writing – review & editing, Supervision, Project administration, Funding acquisition. **Ján Lakota:** Writing – review & editing, Supervision, Funding acquisition.

Ondrej Šauša: Methodology, Resources, Writing – review & editing, Supervision, Project administration, Funding acquisition.

Data availability

Data will be made available on request.

Declaration of Competing Interest

The authors declare that they have no known competing financial interests or personal relationships that could have appeared to influence the work reported in this paper.

Acknowledgments

The research was funded by the APVV agency (project no. SK-BY-RD-19-0019, and APVV-21-0335), VEGA agency (project no. 2/0134/21 and 2/0166/22), KEGA agency (project no. 041UK-4/2020) and Foundation for Cell Transplantation.

References

- [1] Y. Naaldijk, A.A. Johnson, A. Friedrich-Stöckigt, A. Stolzinger, Cryopreservation of dermal fibroblasts and keratinocytes in hydroxyethyl starch-based cryoprotectants, *BMC Biotechnol.* 16 (1) (2016) 1–11, <https://doi.org/10.1186/s12896-016-0315-4>.
- [2] J.N. Kearney, Cryopreservation of cultured skin cells, *Burns*. 17 (5) (1991) 380–383, [https://doi.org/10.1016/S0305-4179\(05\)80070-1](https://doi.org/10.1016/S0305-4179(05)80070-1).
- [3] J. Corsini, F. Maxwell, I.H. Maxwell, Storage of Various Cell Lines at -70°C or -80°C in Multi-Well Plates While Attached to the Substratum, *Biotechniques*. 33 (1) (2002) 42–46, <https://doi.org/10.2144/02331bm05>.
- [4] S.R. May, S.K. Rudis, C.A. Rubin, Optimum cooling and warming rates for the cryopreservation of cultured human keratinocytes and mouse L cells, *Cryobiology*. 25 (6) (1988) 516–517, [https://doi.org/10.1016/0011-2240\(88\)90321-5](https://doi.org/10.1016/0011-2240(88)90321-5).
- [5] T. Fujita, Y. Takami, K. Ezoe, et al., Successful preservation of human skin by vitrification, *Journal of Burn Care & Rehabilitation*. 021 (4) (2000), <https://doi.org/10.1067/jmbc.2000.107745>.
- [6] L.H. Campbell, K.G.M. Brockbank, Development of a Vitrification Preservation Process for Bioengineered Epithelial Constructs, *Cells*. 11 (7) (2022), <https://doi.org/10.3390/cells11071115>.
- [7] J. Pasch, A. Schiefer, I. Heschel, G. Rau, Cryopreservation of keratinocytes in a monolayer, *Cryobiology*. 39 (2) (1999) 158–168, <https://doi.org/10.1006/cryo.1999.2197>.
- [8] P. Mazur, Freezing of living cells: mechanisms and implications, *Am J Physiol*. 247 (3 Pt 1) (1984) C125–C142, <https://doi.org/10.1152/ajpcell.1984.247.3.C125>.
- [9] J.E. Lovelock, The haemolysis of human red blood-cells by freezing and thawing, *Biochim Biophys Acta*. 10 (1953) 414–426, [https://doi.org/10.1016/0006-3002\(53\)90273-X](https://doi.org/10.1016/0006-3002(53)90273-X).
- [10] P. Mazur, S.P. Leibo, E.H.Y. Chu, A two-factor hypothesis of freezing injury, *Exp Cell Res.* 71 (2) (1972) 345–355, [https://doi.org/10.1016/0014-4827\(72\)90303-5](https://doi.org/10.1016/0014-4827(72)90303-5).
- [11] S. Zawlodzka, H. Takamatsu, Osmotic injury of PC-3 cells by hypertonic NaCl solutions at temperatures above 0°C, *Cryobiology*. 50 (1) (2005) 58–70, <https://doi.org/10.1016/j.cryobiol.2004.10.004>.
- [12] A.M.M. Zade-Oppen, Posthypertonic Hemolysis in Sodium Chloride Systems, *Acta Physiol Scand.* 73 (3) (1968) 341–364, <https://doi.org/10.1111/j.1748-1716.1968.tb04113.x>.
- [13] P. Mazur, K.W. Cole, Roles of unfrozen fraction, salt concentration, and changes in cell volume in the survival of frozen human erythrocytes, *Cryobiology*. 26 (1) (1989) 1–29, [https://doi.org/10.1016/0011-2240\(89\)90030-8](https://doi.org/10.1016/0011-2240(89)90030-8).
- [14] H. Takamatsu, S. Zawlodzka, Contribution of extracellular ice formation and the solution effects to the freezing injury of PC-3 cells suspended in NaCl solutions, *Cryobiology*. 53 (1) (2006) 1–11, <https://doi.org/10.1016/j.cryobiol.2006.03.005>.
- [15] B. Han, J.C. Bischof, Direct cell injury associated with eutectic crystallization during freezing, *Cryobiology*. 48 (1) (2004) 8–21, <https://doi.org/10.1016/j.cryobiol.2003.11.002>.
- [16] I. Klbik, K. Čechová, S. Milovská, et al., Cryoprotective Mechanism of DMSO Induced by the Inhibitory Effect on Eutectic NaCl Crystallization, *J Phys Chem Lett.* 13 (48) (2022) 11153–11159, <https://doi.org/10.1021/acs.jpcclett.2c03003>.
- [17] Z. Yuan, S.D.S. Lourenco, E.K. Sage, K.K. Kolluri, M.W. Lowdell, S.M. Janes, Cryopreservation of human mesenchymal stromal cells expressing TRAIL for human anti-cancer therapy, *Cytotherapy*. 18 (7) (2016) 860–869, <https://doi.org/10.1016/j.jcyt.2016.04.005>.
- [18] S. Thirumala, J.M. Gimble, R. Devireddy v, Evaluation of methylcellulose and dimethyl sulfoxide as the cryoprotectants in a serum-free freezing media for

- cryopreservation of adipose-derived adult stem cells, *Stem Cells Dev.* 19 (4) (2010) 513–522, <https://doi.org/10.1089/scd.2009.0173>.
- [19] J. Lakota, P. Fuchsberger, Autologous stem cell transplantation with stem cells preserved in the presence of 4.5 and 2.2% DMSO, *Bone Marrow Transplant.* 18 (1) (1996) 262–263.
- [20] K. Čechová, I. Maňko, J. Rusnák, et al., Microstructural free volume and dynamics of cryoprotective DMSO–water mixtures at low DMSO concentration, *RSC Adv.* 9 (59) (2019) 34299–34310, <https://doi.org/10.1039/C9RA06305F>.
- [21] B.P. Best, Cryoprotectant Toxicity: Facts, Issues, and Questions, *Rejuvenation Res.* 18 (5) (2015) 422–436, <https://doi.org/10.1089/rej.2014.1656>.
- [22] M. Awan, I. Buriak, R. Fleck, et al., Dimethyl sulfoxide: a central player since the dawn of cryobiology, is efficacy balanced by toxicity?, *Regenerative Med* 15 (3) (2020) 1463–1491, <https://doi.org/10.2217/rme-2019-0145>.
- [23] D.Y. Gao, J. Liu, C. Liu, et al., Andrology: Prevention of osmotic injury to human spermatozoa during addition and removal of glycerol*, *Human Reproduction.* 10 (5) (1995) 1109–1122, <https://doi.org/10.1093/oxfordjournals.humrep.a136103>.
- [24] K. Kehe, M. Abend, K. Kehe, R. Ridi, R.U. Peter, D. van Beuningen, Tissue engineering with HaCaT cells and a fibroblast cell line, *Arch Dermatol Res.* 291 (11) (1999) 600–605, <https://doi.org/10.1007/s004030050461>.
- [25] B. qiu Li, X. Dong, S hong Fang, J you Gao, G. qin Yang, H. Zhao, Systemic toxicity and toxicokinetics of a high dose of polyethylene glycol 400 in dogs following intravenous injection, *Drug Chem Toxicol.* 34 (2) (2011) 208–212, <https://doi.org/10.3109/01480545.2010.500292>.
- [26] V.S. Chadwick, S.F. Phillips, A.F. Hoffmann, Measurements of intestinal permeability using low molecular weight polyethylene glycols (PEG 400). I. Chemical analysis and biological properties of PEG 400, *Gastroenterology.* 73 (2) (1977) 241–246, [https://doi.org/10.1016/s0016-5085\(19\)32196-1](https://doi.org/10.1016/s0016-5085(19)32196-1).
- [27] G. Liu, Y. Li, L. Yang, et al., Cytotoxicity study of polyethylene glycol derivatives, *RSC Adv.* 7 (30) (2017) 18252–18259, <https://doi.org/10.1039/c7ra00861a>.
- [28] N.S. Pushkar, G.S. Lobytseva, Y.P. Timoshenko, Low-temperature preservation of bone marrow with PEO-400, *Cryobiology.* 15(6):699 (1978), [https://doi.org/10.1016/0011-2240\(78\)90149-9](https://doi.org/10.1016/0011-2240(78)90149-9).
- [29] V. Lemesheko v, V.A. Bondarenko, N.P. Subota, A.M. Belous, Cryoinjury and cryoprotection of mitochondria in vitro and in situ, *Problems of Cryobiology and Cryomedicine.* 2):33–37 (1976).
- [30] L. Huang, K. Nishinari, Interaction between poly(ethylene glycol) and water as studied by differential scanning calorimetry, *J Polym Sci B Polym Phys.* 39 (5) (2001) 496–506, [https://doi.org/10.1002/1099-0488\(20010301\)39:5<496::AID-POLB1023>3.0.CO;2-H](https://doi.org/10.1002/1099-0488(20010301)39:5<496::AID-POLB1023>3.0.CO;2-H).
- [31] A.D. Fortes, J. Ponsonby, O. Kirichek, V. García-Sakai, On the crystal structures and phase transitions of hydrates in the binary dimethyl sulfoxide–water system, *Acta Crystallogr B Struct Sci Cryst Eng Mater.* 76 (2020) 733–748, <https://doi.org/10.1107/S2052520620008999>.
- [32] O.K. Gulevskiy, Influence of cryoprotective agents on protein biosynthesis in Krebs-2 ascites carcinoma and wheat germ cell-free systems, *Cryobiology.* 96 (February) (2020) 55–60, <https://doi.org/10.1016/j.cryobiol.2020.08.005>.
- [33] Pegg DE, Diaper MP. The “Unfrozen Fraction” Hypothesis of Freezing Injury to Human Erythrocytes: A Critical Examination of the Evidence. Vol 26.; 1989.
- [34] H. Ishiguro, B. Rubinsky, Mechanical Interactions between Ice Crystals and Red Blood Cells during Directional Solidification, *Cryobiology.* 31 (5) (1994) 483–500, <https://doi.org/10.1006/cryo.1994.1059>.
- [35] M. Toner, E.G. Cravalho, M. Karel, D.R. Arment, Cryomicroscopic analysis of intracellular ice formation during freezing of mouse oocytes without cryoadditives, *Cryobiology.* 28 (1) (1991) 55–71, [https://doi.org/10.1016/0011-2240\(91\)90008-C](https://doi.org/10.1016/0011-2240(91)90008-C).
- [36] A. Hubel, T.B. Darr, A. Chang, J. Dantzig, Cell partitioning during the directional solidification of trehalose solutions, *Cryobiology.* 55 (3) (2007) 182–188, <https://doi.org/10.1016/j.cryobiol.2007.07.002>.
- [37] A.I. Osetsky, A.L. Kirilyuk, T.M. Gurina, On Possible Mechanism of Damage in Frozen-Thawed Biological Objects Due to Pressure Plastic Relaxation in Closed Liquid Phase Inclusions, *Problems of Cryobiology and Cryomedicine.* 17 (3) (2007) 272–282. <http://journal.cryo.org.ua/index.php/probl-cryobiol-cryomed/article/view/502>.
- [38] H. Takamatsu, B. Rubinsky, Viability of deformed cells, *Cryobiology.* 39 (3) (1999) 243–251, <https://doi.org/10.1006/cryo.1999.2207>.
- [39] E. Szél, J. Danis, E. Sörös, et al., Protective effects of glycerol and xylitol in keratinocytes exposed to hyperosmotic stress, *Clin Cosmet Investig Dermatol.* 12 (2019) 323–331, <https://doi.org/10.2147/CCID.S197946>.
- [40] D. Arbelaez-Camargo, M. Roig-Carreras, E. García-Montoya, et al., Osmolality predictive models of different polymers as tools in parental and ophthalmic formulation development, *Int J Pharm.* 543 (1–2) (2018) 190–200, <https://doi.org/10.1016/j.ijpharm.2018.03.052>.
- [41] I. Kratochvílová, M. Golan, K. Pomeisl, et al., Theoretical and experimental study of the antifreeze protein AFP752, trehalose and dimethyl sulfoxide cryoprotection mechanism: correlation with cryopreserved cell viability, *RSC Adv.* 7 (1) (2017) 352–360, <https://doi.org/10.1039/C6RA25095E>.
- [42] B.J. Fuller, N. Lane, E.E. Benson (Eds.), *Life in the Frozen State*, CRC Press, 2004, <https://doi.org/10.1201/9780203647073>.
- [43] W. Liu, Z. Huang, B. Liu, et al., Investigating solution effects injury of human T lymphocytes and its prevention during interrupted slow cooling, *Cryobiology.* 99 (2021) 20–27, <https://doi.org/10.1016/j.cryobiol.2021.01.018>.
- [44] J. Pasch, A. Schiefer, I. Heschel, N. Dimoudis, G. Rau, Variation of the HES concentration for the cryopreservation of keratinocytes in suspensions and in monolayers, *Cryobiology.* 41 (2) (2000) 89–96, <https://doi.org/10.1006/cryo.2000.2270>.
- [45] A. Ito, K. Yoshioka, S. Masumoto, et al., Magnetic heating of nanoparticles as a scalable cryopreservation technology for human induced pluripotent stem cells, *Sci Rep.* 10 (1) (2020) 1–12, <https://doi.org/10.1038/s41598-020-70707-6>.
- [46] S.Y. Chuang, Positron Annihilation and Phase Transitions in Molecular Substances, *Chinese Journal of Physics.* 16 (2–3) (1978). <https://scholars.lib.ntu.edu.tw/bitstream/123456789/32431/1/0111.pdf>.
- [47] M. Eldrup, D. Lightbody, J.N. Sherwood, Studies of phase transformations in molecular crystals using the positron annihilation technique, *Faraday Discuss Chem Soc.* 69 (1980) 175, <https://doi.org/10.1039/dc9806900175>.
- [48] M. Roussanova, M.A. Alam, S. Townrow, et al., A nano-scale free volume perspective on the glass transition of supercooled water in confinement, *New J Phys.* 16 (October) (2014), <https://doi.org/10.1088/1367-2630/16/10/103030>.
- [49] R. Zaleski, M. Gorgol, A. Kiersy, et al., Unraveling the Phase Behavior of Water Confined in Nanochannels through Positron Annihilation, *The Journal of Physical Chemistry C.* 126 (13) (2022) 5916–5926, <https://doi.org/10.1021/acs.jpcc.1c10877>.
- [50] B. Zgardzińska, M. Paluch, T. Goworek, Positronium lifetime in supercooled 1-butanol: Search for polyamorphism, *Chem Phys Lett.* 491 (4–6) (2010) 160–163, <https://doi.org/10.1016/j.cplett.2010.03.034>.
- [51] R. Kasada, K. Sato, Positron annihilation study on the phase transition of thermally aged Fe–Cr binary alloys at 748K, *Philos Mag Lett.* 99 (10) (2019) 360–371, <https://doi.org/10.1080/09500839.2019.1695070>.
- [52] H. Švajdlenková, A. Kleinová, O. Šauša, et al., Microstructural study of epoxy-based thermosets prepared by “classical” and cationic frontal polymerization, *RSC Adv.* 10 (67) (2020) 41098–41109, <https://doi.org/10.1039/D0RA08298H>.
- [53] J. Kansy, Microcomputer program for analysis of positron annihilation lifetime spectra, *Nucl Instrum Methods Phys Res A.* 374 (2) (1996) 235–244, [https://doi.org/10.1016/0168-9002\(96\)00075-7](https://doi.org/10.1016/0168-9002(96)00075-7).
- [54] S.M. Sterner, D.L. Hall, R.J. Bodnar, Synthetic fluid inclusions. V. Solubility relations in the system NaCl–KCl–H₂O under vapor-saturated conditions, *Gochim Cosmochim Acta.* 52 (5) (1988) 989–1005, [https://doi.org/10.1016/0016-7037\(88\)90254-2](https://doi.org/10.1016/0016-7037(88)90254-2).
- [55] N. Murase, F. Franks, Salt precipitation during the freeze-concentration of phosphate buffer solutions, *Biophys Chem.* 34 (3) (1989) 293–300, [https://doi.org/10.1016/0301-4622\(89\)80066-3](https://doi.org/10.1016/0301-4622(89)80066-3).
- [56] W.E. Brower, M.J. Freund, M.D. Baudino, C. Ringwald, An hypothesis for survival of spermatozoa via encapsulation during plane front freezing, *Cryobiology.* 18 (3) (1981) 277–291, [https://doi.org/10.1016/0011-2240\(81\)90099-7](https://doi.org/10.1016/0011-2240(81)90099-7).
- [57] K.A. Okrotub, N. Surovtsev v, Raman scattering evidence of hydrohalite formation on frozen yeast cells, *Cryobiology.* 66 (1) (2013) 47–51, <https://doi.org/10.1016/j.cryobiol.2012.11.002>.
- [58] A. Kreiner-Møller, F. Stracke, H. Zimmermann, Hydrohalite spatial distribution in frozen cell cultures measured using confocal Raman microscopy, *Cryobiology.* 69 (1) (2014) 41–47, <https://doi.org/10.1016/j.cryobiol.2014.04.018>.
- [59] C. McCarthy, R.F. Cooper, S.H. Kirby, K.D. Rieck, L.A. Stern, Solidification and microstructures of binary ice–I/hydrate eutectic aggregates, *American Mineralogist.* 92 (10) (2007) 1550–1560, <https://doi.org/10.2138/am.2007.2435>.
- [60] J.E. Tanner, Observations of rapid freezing of salt solutions, *Cryobiology.* 12 (4) (1975) 353–363, [https://doi.org/10.1016/0011-2240\(75\)90008-5](https://doi.org/10.1016/0011-2240(75)90008-5).
- [61] N. Murase, P. Echlin, F. Franks, The structural states of freeze-concentrated and freeze-dried phosphates studied by scanning electron microscopy and differential scanning calorimetry, *Cryobiology.* 28 (4) (1991) 364–375, [https://doi.org/10.1016/0011-2240\(91\)90043-N](https://doi.org/10.1016/0011-2240(91)90043-N).
- [62] Selvarajan A. Raman spectrum of dimethyl sulfoxide (DMSO) and the influence of solvents. *Proceedings of the Indian Academy of Sciences - Section A.* 1966;64 (1):44–50. doi:10.1007/BF03049330.
- [63] B. Yang, X. Cao, C. Wang, S. Wang, C. Sun, Investigation of hydrogen bonding in Water/DMSO binary mixtures by Raman spectroscopy, *Spectrochim Acta A Mol Biomol Spectrosc.* 228 (2020), <https://doi.org/10.1016/j.saa.2019.117704>.
- [64] W.N. Martens, R.L. Kristof, K.J. Theo, Raman spectroscopy of dimethyl sulphoxide and deuterated dimethyl sulphoxide at 298 and 77 K, *Journal of Raman Spectroscopy.* 33 (2) (2002) 84, <https://doi.org/10.1002/jrs.827.abs>.
- [65] R.W. Berg, Raman detection of hydrohalite formation: Avoiding accidents on icy roads by deicing where salt will not work, *Appl Spectrosc Rev.* 53 (6) (2018) 503–515, <https://doi.org/10.1080/05704928.2017.1396540>.
- [66] H. Matsuura, K. Fukuhara, Conformational analysis of poly(oxyethylene) chain in aqueous solution as a hydrophilic moiety of nonionic surfactants, *J Mol Struct.* 126 (1985) 251–260, [https://doi.org/10.1016/0022-2860\(85\)80118-6](https://doi.org/10.1016/0022-2860(85)80118-6).
- [67] E.A. Sagitova, K.A. Prokhorov, G.Y. Nikolaeva, et al., Raman analysis of polyethylene glycols and polyethylene oxides, *J Phys Conf Ser.* 999 (1) (2018), <https://doi.org/10.1088/1742-6596/999/1/012002>.
- [68] W. Guo, L. Zhao, X. Gao, Z. Cao, Q. Wang, Accurate quantification of hydration number for polyethylene glycol molecules, *Chinese Physics B.* 27 (5) (2018), <https://doi.org/10.1088/1674-1056/27/5/055101>.
- [69] I. Klibik, K. Čechová, I. Maňko, J. Lakota, O. Šauša, On crystallization of water confined in liposomes and cryoprotective action of DMSO, *RSC Adv.* 12 (4) (2022) 2300–2309, <https://doi.org/10.1039/D1RA08935H>.
- [70] O. Šauša, M. Iskrova, B. Sláviková, V. Majerník, J. Křišťák, Positron Annihilation in Undercooled Water and Ice, *Materials Science Forum.* 666 (2010) 115–118, <https://doi.org/10.4028/www.scientific.net/MSF.666.115>.

- [71] N. Bui-Xuan-Nguyen, Y. Heyman, J.P. Renard, Direct freezing of cattle embryos after partial dehydration at room temperature, *Theriogenology*. 22 (4) (1984) 389–399, [https://doi.org/10.1016/0093-691X\(84\)90459-X](https://doi.org/10.1016/0093-691X(84)90459-X).
- [72] J.P. Renard, G.V. Bui-Xuan-Nguyen, Two-step freezing of two-cell rabbit embryos after partial dehydration at room temperature, *Reproduction*. 71 (2) (1984) 573–580, <https://doi.org/10.1530/jrf.0.0710573>.
- [73] H. Huang, G. Zhao, Y. Zhang, J. Xu, T.L. Toth, X. He, Predehydration and Ice Seeding in the Presence of Trehalose Enable Cell Cryopreservation, *ACS Biomater Sci Eng.* 3 (8) (2017) 1758–1768, <https://doi.org/10.1021/acsbiomaterials.7b00201>.
- [74] L. Shen, X. Guo, X. Ouyang, Y. Huang, D. Gao, G. Zhao, Fine-tuned dehydration by trehalose enables the cryopreservation of RBCs with unusually low concentrations of glycerol, *J Mater Chem B*. 9 (2) (2021) 295–306, <https://doi.org/10.1039/d0tb02426k>.